RES. LAB. REPRINT 3977

GENERAL ELECTRIC
Research Laboratory

THE INTERPLAY OF ELECTRONICS AND VACUUM TECHNOLOGY

BY

J. M. LAFFERTY AND T. A. VANDERSLICE

SCHENECTADY, NEW YORK

THE INTERPLAY OF ELECTRONICS AND VACUUM TECHNOLOGY

BY

J. M. LAFFERTY AND T. A. VANDERSLICE

Reprinted from the PROCEEDINGS OF THE IRE
VOL. 49, NO. 7, JULY, 1961

PRINTED IN THE U.S.A.

The Interplay of Electronics and Vacuum Technology*

J. M. LAFFERTY†, FELLOW, IRE, AND T. A. VANDERSLICE†

Summary—Historically, vacuum technology has played an important part in the development of electron tubes. The operating characteristics of many early devices were dependent on the degree of vacuum obtained. The Roentgen X-ray tube and the Braun cathode-ray tube are examples of these. Improvement in vacuum technology made possible the development of many truly high-vacuum devices in which performance is independent of the inclosed gas pressure. Many modern electronic components no longer operate in a vacuum but are dependent on vacuum technology in their fabrication. These include microminiature circuit elements, cryotrons, photoconductor-electroluminescent devices and ferromagnetic memory systems—all dependent on vacuum evaporated films. Electronic components have also played an important part in the development of modern vacuum technology. These include thermistor gauges, electronic ionization gauges, ion pumps and electronic leak-detection equipment. This paper is devoted to a review of modern ultra-high vacuum systems and the electronic components used in them.

Introduction

HISTORICALLY, vacuum technology has played an important part in the development of electron tubes. The quality and life of these devices have been dependent on the ability to produce and maintain a high vacuum in them. In many of the early tubes, it was impossible to obtain a high vacuum. This led to the development of tubes which were, in many cases, dependent on some gas being present for their successful operation. The presence of gas in the tube placed a serious limitation on the voltage which could be applied without complete breakdown. An example of this is the cold-cathode X-ray tube. The characteristics of the early Roentgen "gas" X-ray tube depended markedly on the gas pressure in the tube. The electron stream in these tubes was produced by a low-pressure gas discharge. The current, applied voltage, and gas pressure were all interdependent. It was not uncommon in those days for a radiologist to use a series of tubes at different gas pressures to produce X rays of various energies or voltages. It was not until the highly evacuated Coolidge tube, with a hot tungsten filament to supply the electrons, was developed that the current could be adjusted independently of the applied voltage. The controllable features of the Coolidge tube have greatly facilitated research and engineering applications of X rays, particularly where precise control is required.

Another tube in which the degree of evacuation has played an important part in its performance is the cathode-ray tube. In the early Braun cathode-ray tube the electrons were liberated and concentrated by means of a gas discharge. The gas present in these early tubes was not dense enough to cause serious scattering of the electrons in the beam, but some of the gas molecules lying in the path of the beam were ionized and formed a positive ion core in the beam. The converging electric field produced by the positive core produced a definite concentrating action on the electron beam. The strength of this focusing action is dependent on the rate of ionization, which in turn depends upon the nature and pressure of the gas and the electron-beam voltage and density. Gas focusing cathode-ray tubes were by necessity slow-speed devices because of the long transit times for the ions. The attainment of a higher degree of vacuum in the cathode-ray tube made possible the development of the modern oxide-coated cathode electron gun by Zworykin in 1933. However, even today, the vacuum technology as practiced in modern cathode-ray television picture-tube processing has not progressed to the point where gas ionization effects are completely absent. Positive ions formed in the beam strike the cathode and limit its life by sputtering. This has been corrected to a large extent by the ion-trap gun. Before the aluminized backing was added to the television picture tube, difficulty was frequently encountered with ion-spot burn of the phosphor in the center of the face plate. This was caused by bombardment of the phosphor by high-velocity negative ions formed by electron attachment.

Electron-beam spread due to space charge is reduced in many modern microwave beam-type tubes by a positive ion core. In many devices this effect is enhanced by adding ion-trap electrodes at the ends of the beam to retain the ions and prevent their draining into the cathode or electron-accelerating region of the device.

Many of our modern electronic components no longer depend on a discharge in vacuum; nevertheless, vacuum technology plays an important part in their manufacture or processing. One of the most important processes is vacuum evaporation of materials for microminiature circuit elements. This involves the evaporation of thin films for passive circuit elements such as resistors and capacitors as well as superconducting films for cryotrons in logic and memory circuits. Vacuum evaporated ferromagnetic films are used in computer memory systems. Several electro-optical elements involving photoconductor-electroluminescent combinations are made by vacuum deposited films. Lack of reproducibility and uniformity in these devices are frequently associated with poor vacuum conditions. In order to maintain uniformity in some of these components which are particularly sensitive to impurities, it is necessary to carry out the evaporation process under ultra-high vacuum conditions at pressures of 10^{-10} mm Hg or better.

* Received by the IRE, February 2, 1961; revised manuscript received, April 17, 1961. The material presented in this paper has been abstracted principally from the revised edition of the late S. Dushman's book, "Scientific Foundations of Vacuum Technique" to be published by John Wiley and Sons, Inc.

† General Electric Research Lab., Schenectady, N. Y.

The testing of electronic components under conditions simulating free space will probably require pressures as low as 10^{-16} mm Hg.

It is interesting to note that, while vacuum technology has historically played an important part in the development of electronic components and will continue to do so in the future, electronic components are playing a role of increasing importance in the development of modern vacuum technology. The modern vacuum system uses semiconducting thermistor gauges for measuring relatively high pressures, electronic ionization gauges for measuring low pressures, and ion pumps for producing low pressures. Leaks are detected in vacuum systems and various other devices by electronic leak detectors using mass spectrometers, scintillation counters, Geiger-Müller tubes, and negative-ion detectors with their associated electronic circuitry.

This paper is devoted to a review of modern ultra-high vacuum systems and the electronic components used in them.

Low Pressure Manometers

Low gas pressures are measured by many different types of gauges. They may be classified, according to the basic principles involved, as follows: 1) Manometers which use mercury or some very nonvolatile liquid. The familiar U-tube manometer, and the well-known McLeod gauge are examples of these. 2) Mechanical manometers which depend on the measurement of the mechanical deformation suffered by a thin wall or diaphragm under pressure. Gauges of this type include the Bourdon spiral and aneroid barometer. 3) Viscosity manometers which depend on the viscous drag in a gas or involve the transfer of momentum by a gas. In the decrement type of viscosity gauge, a surface is set in oscillation and the rate of decrease of amplitude of oscillation is taken as a measure of the pressure. In the rotating disk or molecular gauge, a surface is set in continuous rotation and the amount of twist imparted to an adjacent surface is used to measure the pressure. The molecules striking the moving surface acquire a momentum in the direction of motion which they tend in turn to impart to the other surface. 4) Radiometer-type manometers, which depend on a mechanical force exerted between two surfaces maintained at different temperatures in a gas at low pressure. Instruments of this type are the Crookes radiometer and the Knudsen gauge. In these devices the molecules striking the hotter surface rebound with a higher average kinetic energy than those that strike the colder surface. Consequently, a momentum is imparted to the hot surface which tends to make it move. 5) Heat-conductivity-type manometers, which involve the effect of pressure on the rate of heat transfer. Gauges of this type are the thermocouple gauge, the Pirani resistance gauge and the thermistor gauge. These gauges all depend on the loss of heat from a surface by conduction through the gas at pressures where the distance between the hot and cold surfaces is less than the mean free path. 6) Ionization gauges which depend on the collection and measurement of ions formed by collisions between the gas molecules and high-velocity electrons or other energetic particles.

Fig. 1 shows the approximate operating range of pressure of the gauges just described. Major advances have been made in electronic methods of measuring pressure rather than in mechanical methods. The operating pressure range for ionization gauges has been extended in both directions from about 1 to 10^{-13} mm Hg. As low-pressure measurements have taken on more sophistication there has been a trend towards the use of partial-pressure gauges (mass spectrometers) for the identification of individual gaseous components. These mass spectrometers have taken on a variety of forms from the older magnetic-deflection types with secondary emission multipliers to increase the sensitivity and sweep rate to the more modern time-of-flight instruments and ion-resonance devices using RF fields and strong-focusing quadrupole lenses.

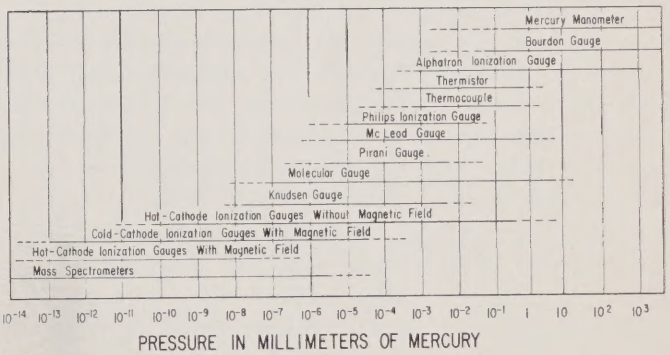

Fig. 1—Chart showing operating pressure ranges for different types of gauges.

Triode Gauges

The ionization gauge, in the form of a simple triode tube structure, is one of the oldest [1], [2] and still most widely used devices for measuring gas pressure under high-vacuum conditions. In this gauge, electrons from a thermionic cathode are accelerated through a positive grid structure. If the accelerating voltage is greater than the ionizing potential of the gas, there is a finite probability that the electrons will ionize the gas molecules on colliding with them. For a given geometry and constant grid voltage, the number of positive ions formed will be proportional to the gas pressure, provided the pressure is so low that any one electron does not make more than one ionizing collision during its flight. The number of positive ions produced is also proportional to the electron emission, provided space charge effects are negligible and do not alter the potential distribution in the gauge. A constant fraction of the ions produced is collected by an electrode which usually surrounds the grid and is negative with respect to the cathode. A measure of the resulting ion current gives an indication of the gas pressure. Let I_p denote the positive-ion current

to the ion collector, I_e the electron-emission current to the grid or anode, and P the gas pressure in the ionization gauge at some standard temperature. Then under the operating conditions discussed above

$$I_p = SI_eP \quad \text{or} \quad P = \frac{1}{S}\frac{I_p}{I_e}, \tag{1}$$

where the proportionality constant S is called the sensitivity of the gauge. If I_p and I_e are measured in the same units, S has the dimensions of reciprocal pressure. Obviously the sensitivity will depend on the nature of the gas present and the electrode geometry and voltages.

It is not uncommon for a triode ionization gauge, such as the VG-1A, shown in Fig. 2, for example, to have a sensitivity of $S = 20$/mm Hg for nitrogen. At a pressure of 10^{-6} mm Hg, substitution in (1) shows that only one ion is produced by every 50,000 electrons that travel from the cathode to the anode. The factors which affect the low-pressure limit of the triode gauge are discussed in the next section on gauges for ultra-high vacuums.

The upper pressure limit for most triode ionization gauges is about a micron. At higher pressures the ion current saturates, leveling off at a constant value independent of pressure. This is due to several effects. At high pressures the mean free path of the electrons between collisions with the gas molecules becomes comparable with the path length normally traveled by the electrons in going from the filament to the grid. Under these conditions the energy lost by the electrons in nonionizing inelastic collisions becomes important. The velocity of the electrons is reduced resulting in lower ionizing efficiencies during the latter part of their flight. The *effective* ionization potential [3] expressed in electron volts or average energy lost by the electrons per ionizing collision may well be equal to nearly half their initial kinetic energy of 150 ev.

The low-energy secondary electrons produced by ionizing collisions in a triode ionization gauge are, in most cases, not effective in producing further ionization. However, these electrons will be collected by the anode and measured with electrons emitted by the filament. If the total electron current to the grid is held constant during the operation of the gauge, as is often the case, the apparent gauge sensitivity will start to drop when these secondary electrons become comparable with the number of electrons emitted by the filament. It can be seen, by substituting numerical values in (1), that for the VG-1A with a sensitivity of $S = 20$/mm Hg, the ion current, and hence, the secondary electron current would just be equal to the electron-emission current at a pressure of 5×10^{-2} mm Hg, if the gauge could retain its sensitivity at this pressure. Actually, when the pressure becomes greater than a few microns, positive-ion space charge builds up around the cathode and an arc-like discharge is established. Under these conditions a characteristic glow may be observed in the gauge. The ion collector becomes a probe immersed in a plasma and collects the random ion current arriving at the sheath surrounding it. This current is no longer dependent on the pressure and cathode emission current in the usual way.

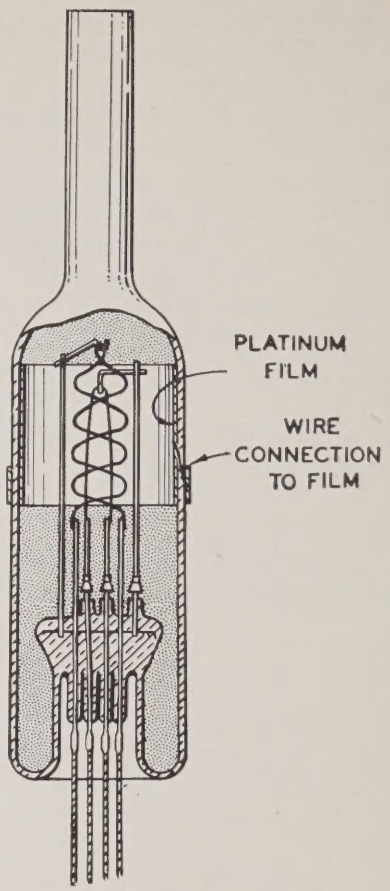

Fig. 2—The VG-1A triode ionization gauge. This popular high-vacuum gauge is outgassed by passing current through the grid and filament and by torching the envelope. The ion collector is a metallic film deposited on the wall of the envelope (Morse and Bowie).

Another factor that leads to nonlinearity in an ionization gauge at high pressures is a decrease in the ion collection efficiency. At high pressures the ions may be scattered to other electrodes before reaching the collector. This results in a smaller fraction of the total ions produced being collected by the ion collector.

Schulz and Phelps [4] have designed a high-pressure ionization gauge that takes these factors into account. Their gauge, the Westinghouse WX4145, shown in Fig. 3, operates in the approximate pressure range of 10^{-5} to 1 mm Hg. It has been used for measuring the pressure of chemically active gases as well as rare gases. The gauge consists of a 5-mil thoriated iridium filament located halfway between two parallel plates of molybdenum $\frac{3}{8} \times \frac{1}{2}$ inch spaced $\frac{1}{8}$ inch apart. The electrons emitted by the filament pass across the 60-mil gap directly to the anode plate without oscillatory motion.

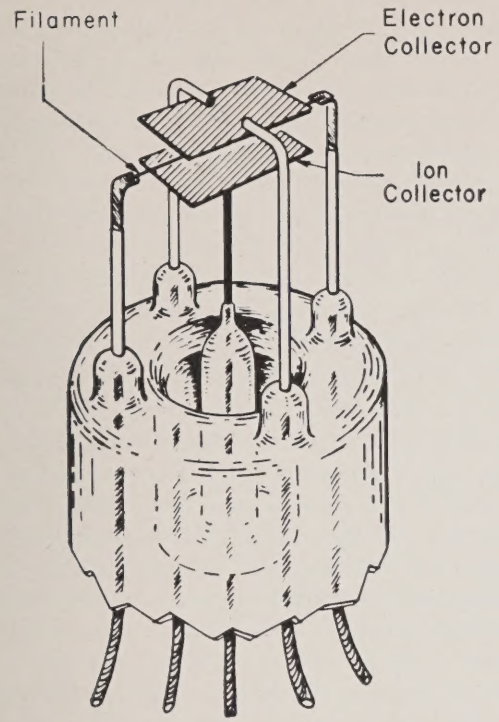

Fig. 3—High-pressure triode ionization gauge (Schulz and Phelps).

This gives the electrons a short path length independent of pressure with little chance of making more than one collision in passing from the filament to the anode. The short path length and the low anode voltage (60 v) give the gauge a sensitivity of only 0.6/mm Hg for nitrogen. This limits the secondary electrons produced by ionizing collisions to less than 10 per cent of the electron-emission current, even at pressures of 0.15 mm Hg. To insure efficient ion collection, the ion-collector electrode is made large compared to the filament, and its potential is adjusted to -60 v to assure parallel plane equipotential surfaces between the electrodes.

Philips Ionization Gauge

Many of the difficulties associated with chemically active gases reacting with the filament in the hot-cathode ionization gauges have been overcome by the Philips ionization manometer developed by Penning [5]. In this gauge, electrons are ejected from a cold cathode of zirconium, thorium, or other active surface by bombardment with positive ions which have been accelerated by passage through the cathode fall of potential. These secondary electrons are deflected by means of a magnetic field so that they travel in long helical paths before reaching the anode. The total length of path traveled by the electrons in going from the cathode to the anode is many hundreds of times the direct distance between the two electrodes. As a result, the ionization produced per electron at any given pressure is considerably greater than would be obtained in the absence of a magnetic field. The magnitude of the total discharge current, which is the sum of the positive-ion current to the cathode and the electron current from the same electrode, is used as a measure of the pressure of gas present.

Fig. 4 shows the construction of the gauge. The manometer tube M contains a ring-shaped anode R located between the cathode plates P. The magnetic field (about 370 oersteds) is applied by means of the permanent magnet H. A microammeter (to measure the current) and 1 megohm resistance are connected in series with the manometer across a dc source of about 2000 v.

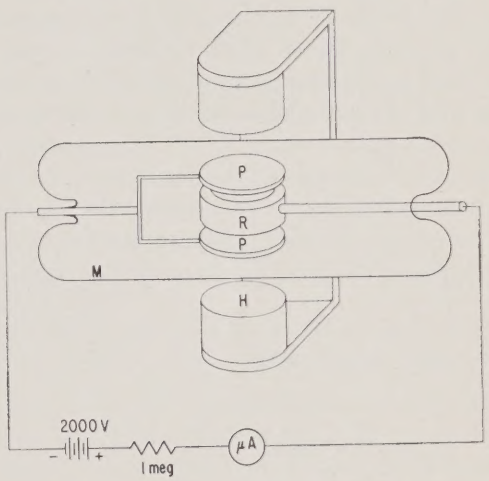

Fig. 4—Philips cold-cathode ionization gauge (Penning).

The Penning gauge does not have the accuracy of the hot-cathode triode gauge. Unstable oscillations generally occur in the glow discharge, and cause unpredictable jumps in the calibration curve. These discontinuities appear to be present in all gauges of this type, and may be as high as 10 per cent. In a later version of the gauge, Penning and Nienhauis [6] have improved the stability by replacing the ring anode with a cylinder.

Penning gauges operate over a pressure range of about 10^{-2} to 10^{-5} mm Hg. At lower pressures it becomes difficult to initiate the discharge, and in some cases it may fail completely to strike. The discharge in the Penning gauge removes gas from the sytem by processes that are discussed in a later section on ion pumps. This causes the gauge to act as a pump and disturbs the pressure distribution in the system. The rate at which gas is pumped by these cold-cathode discharge gauges is from 10 to 100 times greater than that of a hot-cathode triode gauge. For this reason they should be provided with a large tubulation with adequate conductance to prevent a pressure drop between the gauge and the vacuum system. Notwithstanding these disadvantages, the Penning gauge has found wide applications because of its simplicity and ruggedness.

Radioactive Ionization Gauges

A novel type of cold-cathode gauge was developed by Downing and Mellen [7] in the laboratories of the NRC Equipment Corporation of Newton, Mass.; it was designated the "Alphatron," to indicate that the ionization is produced by alpha particles. Fig. 5 shows a schematic diagram of the ionization chambers and electrical circuit. A dc potential of 108 v is applied between the ionization chambers and the ion collectors. The very small ionization current, produced by the alpha particles from the radium sources, is greatly amplified so that it can be read on a standard type of microammeter. The dc voltage, as well as the power for operating the amplifier, is obtained from the regular ac 60-cycle, 110-volt supply. The radium sources are so constructed that a small quantity of radium in equilibrium with its disintegration products, radon, radium A, radium B, and so forth, radiates alpha particles at a constant rate. Since radon, the first distintegration product of radium, is a gas, the source must be sealed in a plaque to prevent the loss of radon gas so that the succeeding products may be held in the source and their alpha activity utilized.

By using two ionization chambers, the Model 530 Alphatron gauge is made to operate with a linear response for air from 10^{-3} to 10^{3} mm Hg. The large chamber has a volume of 51 cc and with a radium source of 100 microcuries has a sensitivity for air of about 10^{-10} a/mm Hg. In the three high-pressure ranges from 10 to 1000 mm Hg the small ionization chamber is used in order to keep ionization current loss down due to volume recombination. The small chamber has a volume of 0.2 cc, and with a radium source of 1.5 microcuries has a sensitivity for air of about 1.5×10^{-13} a/mm Hg.

The sensitivity of the Alphatron depends on the kind of gas being measured. Conversion factors for the more common gases which are to be applied to the output current meter are given in Fig. 6. Due to recombination, the readings for gases heavier than air are not linear in the pressure range of 100 to 1000 mm Hg.

One obvious advantage of this gauge is that there is no filament to burn out and no possibility of chemical reaction between the gas and the cathode. It will also measure higher pressures than the triode ionization gauges. On the other hand, there are certain precautions (discussed very fully in the operating instructions) which have to be carefully attended to in using the gauge, in order to avoid any possible physiological effects arising from the radium emanation.

Spencer and Boggess [8] and their colleagues at the University of Michigan have also developed a radioactive ionization gauge using tritium for the radioactive source.

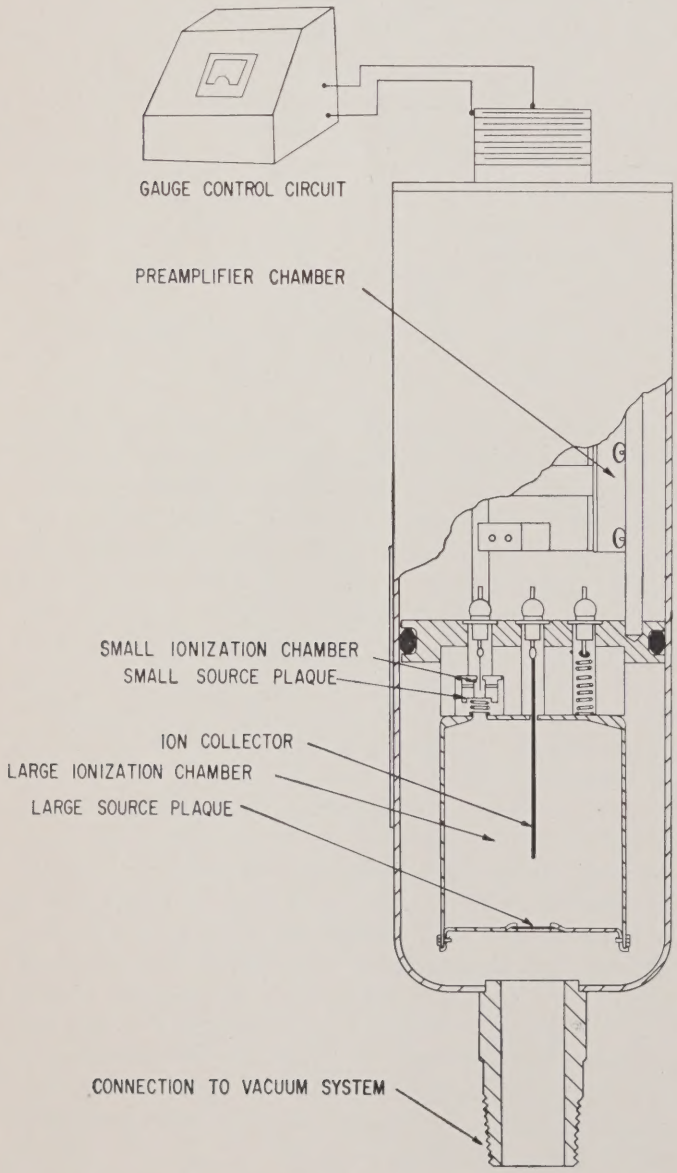

Fig. 5—Schematic sketch of the Alphatron ionization gauge which uses a radioactive source (Downing and Mellen).

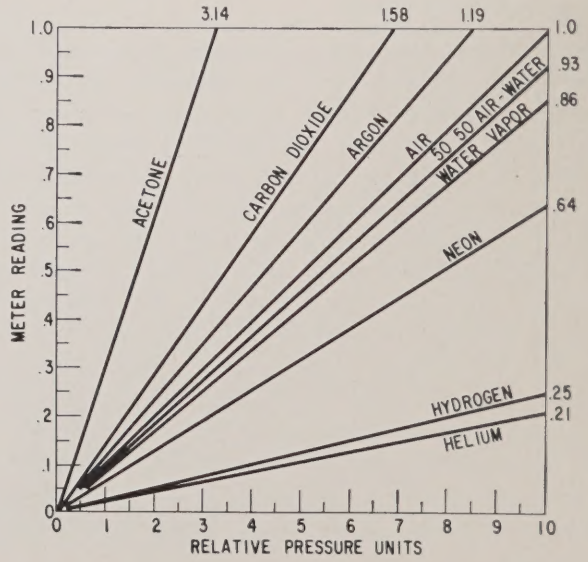

Fig. 6—Relative response of the Alphatron gauge to various gases.

Gauges for Ultra-High Vacuums

The conventional ionization gauge used prior to 1948 was not capable of measuring pressures below about 10^{-8} mm Hg. However, Nottingham and Apker had observed, in attempting to evacuate electronic devices to extremely low pressures, that thermionic and photoelectric emission characteristics indicated pressures much lower than 10^{-8} mm Hg. In 1947, Nottingham [9] presented evidence of a residual current to the ion collector which is completely independent of the pressure. This current is caused by photoelectrons ejected from the ion collector by soft X rays produced by 150-volt electrons striking the grid. Since the photoelectrons *emitted* from the ion collector cannot be distinguished on the current meter from the positive ions *incident* on the collector, there must exist a lower limit to the collector current, with decrease in pressure, which corresponds to pure photoelectric emission. For conventional gauges at normal operating voltages this X-ray photocurrent is about 2×10^{-7} times the anode current. Thus for a gauge with a sensitivity of $S=20$/mm Hg, the ion current to the collector would just be equal to the photoelectric current at a pressure of 10^{-8} mm Hg.

Bayard-Alpert Gauge

A consideration of these problems led Bayard and Alpert [10] in 1950 to develop the inverted ionization gauge shown in Fig. 7. The filament is placed outside the cylindrical grid, and the ion collector, consisting of a very fine wire, is suspended within the grid. The usual potentials are applied to the electrodes, +150 v on the grid and −45 v on the ion collector. Electrons from the filament are accelerated into the grid cylinder where they make ionizing collisions. A large fraction of the ions thus formed inside the grid are collected by the center wire. With this arrangement, the ion collector intercepts only a small fraction of the X rays produced at the grid. The small surface area of the collector wire presents a solid angle to the X rays from the grid that is several hundred times smaller than that for the conventional cylindrical collector.

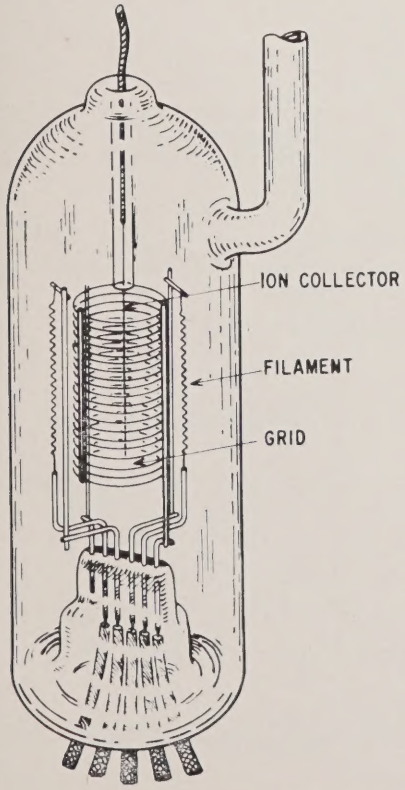

Fig. 7—The inverted triode ionization gauge (Bayard and Alpert).

A unique feature of the Bayard-Alpert gauge is the logarithmic potential distribution in the ionizing region between the cylindrical grid and coaxial ion collector. Since the potential inside the grid is nearly uniform, except in the immediate vicinity of the collector wire, the electrons travel within most of the grid volume with an efficient ionizing energy of nearly 150 ev. This is a distinct advantage over the conventional gauge, where the potential fall approximates a linear distribution between the grid and ion collector. In this case the electrons are decelerated to energies inefficient for ionization over a sizable portion of the volume between the grid and ion collector.

The almost uniform energy of the electrons in the ionizing space of the Bayard-Alpert gauge has allowed Nottingham to identify residual gases by measuring the appearance potential for ionization.

The second filament in the Bayard-Alpert gauge is electrically separated from the first, and not only serves as a spare, but may be used in connection with the flash-filament technique of estimating low gas pressure developed by Apker [11].

The glass sleeve around the ion collector lead prevents X rays from striking the large diameter lead-in wire, and provides a long leakage path between the collector and wall of the gauge which may become charged or electrically conducting from metallic deposits.

Nottingham [12] and Alpert [13] have suggested modifications of the Bayard-Alpert gauge to improve its sensitivity. The cylindrical grid is closed at top and bottom and a second grid, acting as a screen grid, is installed around all the electrodes. The purpose of closing the cylindrical grid is to prevent ions from escaping to the negatively-charged glass wall. At low pressures the ions may oscillate about the collector wire many times before being collected. Since the ions are likely to have velocity components parallel to the collector wire, they may escape through the ends of the grid before being collected unless the grid is closed. The screen grid shields the gauge from the wall charges. Operation of the screen grid at a negative potential causes the electrons to oscillate several times through the positive grid before being collected. This increases their average path length and gives the gauge a higher sensitivity. In some cases the screen grid is made by coating the glass envelope with a conducting film that is connected to an external lead. These improvements have increased the sensitivity by factors of two or three.

Nottingham [14] reported finding that at normal calibrating pressures the ion collector in the modified Bayard-Alpert gauge did not collect a constant fraction of the ions generated inside the grid. He found that for nitrogen at a pressure of 2.4×10^{-3} mm Hg the gauge may be in error by as much as a factor of 2 at emission currents of 100 μa and a factor of 6 at 1 ma. Correct readings are obtained at 10 μa and less. He observed similar effects to a smaller degree in the Bayard-Alpert gauge of type WL-5966. As the gas pressure is reduced the maximum permissible electron current increases inversely with the square root of the pressure. Nottingham suggests that this effect may be due to positive-ion space charge in the vicinity of the ion-collector wire.

The Bayard-Alpert gauge, in the form of the Westinghouse WL-5966, has a sensitivity of $S=12$/mm Hg for nitrogen and has a linear calibration curve over the pressure range of 10^{-9} to 10^{-4} mm Hg. The helium sensitivity is a factor of ten lower. Because of its simplicity of construction, ease of outgassing, and dual filaments, this gauge has found wide acceptance and use by workers in all phases of the high-vacuum field.

Cold-Cathode Inverted Magnetron Gauge

The Penning type of cold-cathode discharge gauge would appear to have certain advantages over the hot-cathode triode ionization gauges for measurement of ultra-high vacuums. There is no limitation on pressure measurements due to X-ray photoemission, since the number of electrons that strike the anode and produce the X rays decreases with the pressure. The vapor pressure of a hot tungsten filament also presents no limitations on the low-pressure limit. However, there are certain inherent disadvantages in the operation of a Penning gauge at pressures below 10^{-5} mm Hg. In most gauges the discharge fails to strike below these pressures. The application of higher voltages to start and maintain the discharge leads to field emission from the ion-collector electrode which cannot be distinguished from ion current by the external measuring circuit. This field-emission current establishes a lower-pressure limit for the operation of the Penning gauge analogous to the X-ray limit for the Bayard-Alpert gauge. To circumvent these difficulties Hobson and Redhead [15] designed an ionization gauge employing a cold-cathode discharge in crossed electric and magnetic fields. Their gauge, shown in Fig. 8, has the structure of an inverted magnetron with an auxiliary cathode. This geometry provides efficient electron trapping in the discharge region, and the auxiliary cathode provides the initial field emission for starting and allows the positive-ion current to be measured independently of the field-emission current. The auxiliary cathode also acts as an electrostatic shield for the ion collector. The two short tubular shields, which project 2 mm into the ion collector from the auxiliary cathode, protect the end plates of the ion collector from the high electric fields and provide the field emission which initiates the discharge.

The gauge operates with an applied magnetic field of 2060 oersteds and a potential of six kv on the anode. Under these conditions the relationship between ion collector current and pressure is given by

$$i_p = cP^n, \tag{2}$$

where i_p is the collector current in amperes, P is the pressure in mm Hg, c is a constant between 1 and 10, and n lies between 1.10 and 1.4 for various gauges. According to Hobson and Redhead, the value of n is essentially independent of the anode voltage, and approaches unity as the magnetic field is increased. The dimensions of the gauge have little effect on the value of n. In the theory of the Townsend discharge applied to the inverted magnetron gauge, Redhead [16] has pointed out that this nonlinear relationship between the ion current and pressure exists because the striking voltage is a slowly varying function of the pressure.

Unlike the triode gauges, the sensitivity ratio of the inverted magnetron gauge for various gases is a function of pressure. The sensitivity ratio for helium to air decreases with pressure and is also a function of the anode voltage.

Oscillations were observed in the inverted magnetron gauge under most operating conditions. Discontinuous jumps in the mode of oscillation from one frequency to another give only small discontinuities in the current-pressure characteristics.

The time lag between the application of anode voltage to the gauge and the initiation of the discharge becomes

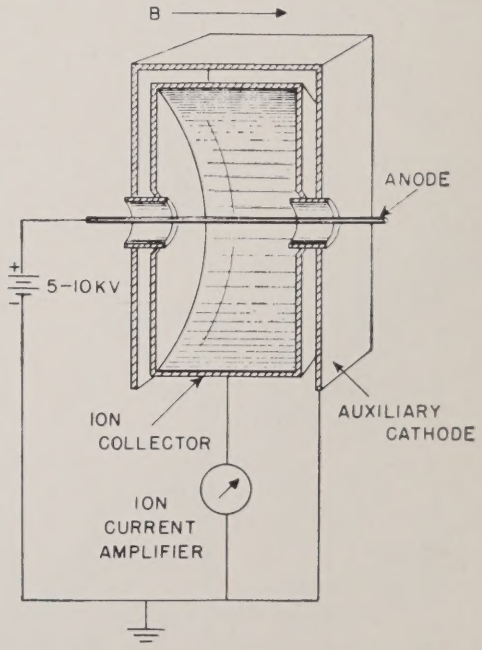

Fig. 8—The cold-cathode inverted magnetron ionization gauge (Hobson and Redhead).

appreciable and variable at pressures below 10^{-8} mm Hg. At pressures near 10^{-12} mm Hg the time lag was as long as ten minutes; however, it is reported that no gauges failed to strike.

A commercial version of this gauge, type 2205-02, is now manufactured by the NRC Equipment Corporation of Newton, Mass. The commercial gauge operates over a pressure range from 10^{-4} to 10^{-12} mm Hg with a sensitivity of 4.5 a/mm Hg for air at 6000 v with a magnetic field strength of 1000 oersteds.

Hot-Cathode Magnetron Ionization Gauge

In order to extend the low-pressure limit of the conventional hot-cathode ionization gauge it is necessary, at a given emission current, to increase the ratio of the ion current to the X-ray photocurrent. As previously explained, this was accomplished in the Bayard-Alpert gauge by reducing the X-ray photocurrent without substantial loss of gauge sensitivity. This ratio may also be increased by increasing the sensitivity of the ionization gauge. It is evident that if the gauge is modified in such a way that the electrons travel in longer paths before they are collected by the positive grid or anode, the probability of their colliding with and ionizing a gas molecule will be greatly enhanced and the sensitivity of the gauge will be improved with no increase in X-ray photoemission. Lafferty [17] has applied this principle in developing a hot-cathode magnetron ionization gauge for ultra-high vacuum use. In this arrangement, shown in Fig. 9, a cylindrical magnetron is operated with a magnetic field greater than cutoff. Two end plates maintained at a negative potential relative to the cathode prevent the escape of electrons. One or both of these plates may be used to collect the positive-ion current generated in the magnetron. Electrons emitted by the tungsten-filament spiral around the axial magnetic field in the region between the negative end plates. If the magnetic field is sufficiently high, most of the electrons fail to reach the anode. Some of the electrons make many orbits around the cathode before being collected. The electron density is therefore increased by the presence of the magnetic field and the probability of ionizing the gas is considerably increased. This is illustrated in Fig. 10, where the ion current to one end plate and the electron current to the anode are plotted as a function of magnetic field for a magnetron gauge with an anode

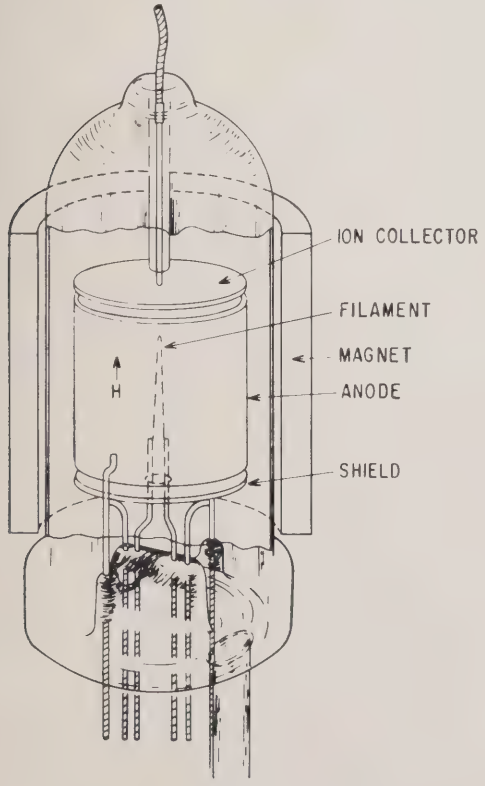

Fig. 9—The hot-cathode magnetron ionization gauge (Lafferty).

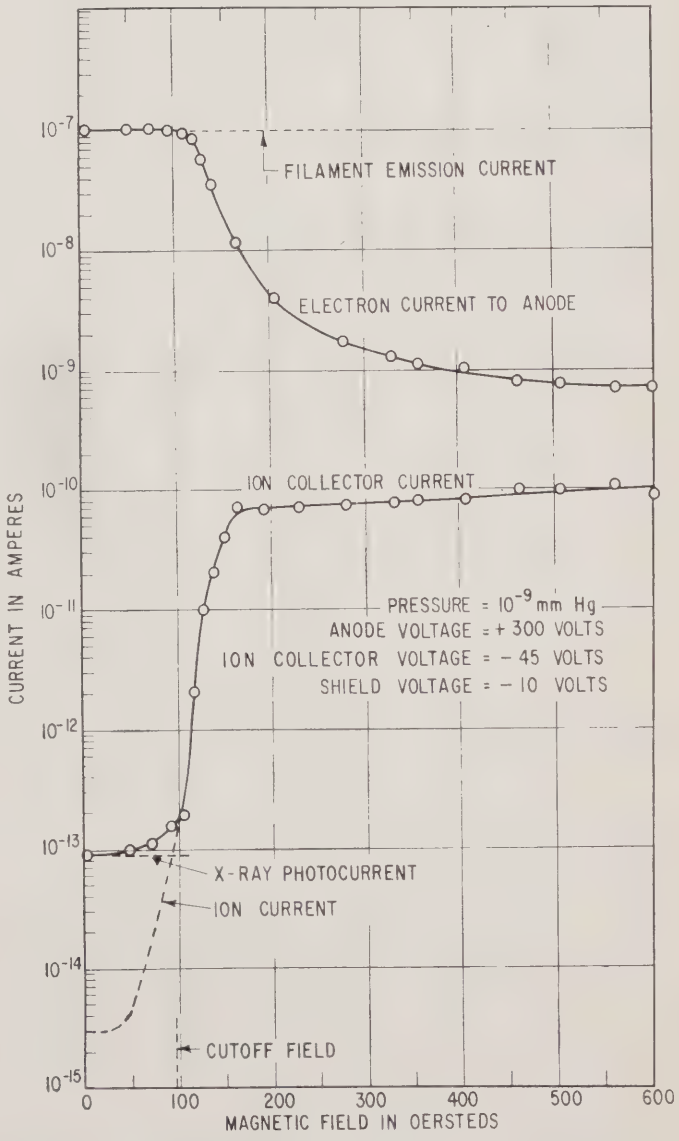

Fig. 10—Ion-collector current and anode electron current as a function of magnetic field for the hot-cathode magnetron gauge.

15/16 inch in diameter and $1\frac{1}{8}$ inches long. The 8-mil hairpin tungsten filament is $\frac{3}{4}$ inch long, separated 40 mils at the base. The filament temperature is adjusted to give an emission current of 10^{-7} a with zero magnetic field. Under these conditions the ion-collector current is nearly 10^{-13} a at a pressure of 10^{-9} mm Hg. However, from measurements made in the 10^{-6} mm Hg pressure range, the sensitivity of the gauge is known to be 30/mm Hg. Thus the true ion current at a pressure of 10^{-9} mm Hg would be only 3×10^{-15} a, as shown by the dotted line in Fig. 10. The actual current measured in the ion-collector circuit is 30 times this value and is essentially all photocurrent produced by X rays from the 300-volt electrons striking the anode. From this it would appear that on the average one photoelectron is emitted by the ion collector for every million electrons striking the anode. As the magnetic field is increased and the electrons begin to miss the anode, their path length is increased. This is indicated by a sharp rise in the ion current and a drop in the electron current collected by the anode. At a magnetic field strength of 250 oersteds, the ion current is enhanced 25,000 times over what it would be without the field, and the electron current collected drops to 1/50 of its former value. The ratio of ion current to X-ray photocurrent is thus increased 1.25×10^{6} times by application of the magnetic field. Since the cut-off current to the anode remains constant independent of pressure at these low pressures, the ion current to the collector would just equal the X-ray photocurrent at a pressure of 2.4×10^{-14} mm Hg. Thus, pressures at least this low could be measured. In practice, the ability to read low pressure is limited by the sensitivity of the external circuit used to measure the ion current.

Hot-cathode magnetron gauges have been shown to have extremely high sensitivities when operated in the ma electron-emission range at pressures of the order of 10^{-5} mm Hg [18]. However, they have always been subject to excessive pumping action and unstable operation frequently associated with oscillations. Lafferty has found that these conditions may be avoided by operating the magnetron gauge at very low electron-emission levels.

Partial-Pressure Gauges

While the ionization gauges give a measure of the total residual pressure of the gases in a vacuum system, there are times when it would be highly desirable to know what these residual gases are. In the hot-plasma experiments related to fusion, it is important to know the purity of the gases involved since the presence of ions of large mass compared to the hydrogen isotopes tend to cool the plasma. Recent interest in determining the neutral and ionic components of the upper atmosphere and beyond has stimulated the design of special equipment for this purpose. Successful rocket and satellite flights have already been made with the Bennett radio-frequency type of mass spectrometer. Many more such devices are sure to follow for space investigations.

Omegatron

The omegatron, originally developed by Sommer, Thomas, and Hipple [19] for measuring atomic constants, has been used by Alpert and Buritz [20] as a mass spectrometer for measuring the partial pressures of the various gases in an ultra-high vacuum system. A simplified version of the omegatron capable of high-temperature outgassing as developed by Alpert and Buritz is shown in Fig. 11.

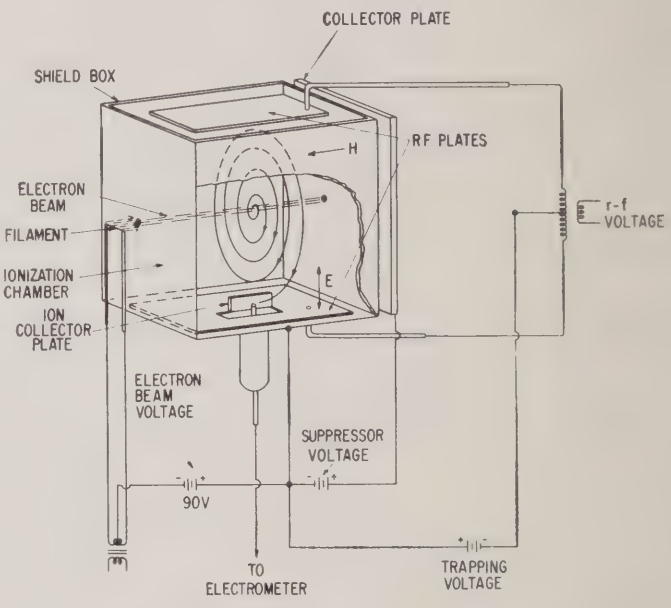

Fig. 11—Schematic diagram of a simplified version of the omegatron (Sommer, Thomas, and Hipple) developed by Alpert and Buritz.

The operation of the omegatron is similar to that of the cyclotron. Electrons emitted from the hot filament are accelerated through a 1/16-inch-diameter aperture to form a 4-μa beam at 90 v. This beam, which produces ions in the ionization chamber, emerges through a second aperture and is collected by a collector plate biased positively with respect to the shield to suppress secondary emission. The parallel magnetic field H has a strong collimating action on the electron beam. The shield box forms a 2-cm cube. The RF plates, which form the top and bottom of the ionization chamber, are connected to a source of RF voltage (about one or two volts). These plates produce an RF field E across the ionization chamber perpendicular to the magnetic field. Ions formed by electrons colliding with the gas molecules within the electron beam are caused to spiral around the magnetic lines of force by their own thermal and dissociation energies. The radii of these spirals are very small and few ions would normally escape from the electron beam due to their own initial energy. However, the applied weak electric RF field causes the ions to be accelerated in Archimedes-like spiral orbits of increasing size provided the frequency of the applied RF voltage is the same as the cyclotron frequency of the ions. A trapping voltage that is positive with respect to the RF

plates is applied to the shield box to produce an electric field which retards the loss of ions in the axial direction of the magnetic field. This gives the RF field an opportunity to act on the ions over a greater number of cycles. The spiral orbits terminate on a 1/16-inch-square ion-collector plate. The ion current to this electrode, detected by a vibrating-reed electrometer, is a measure of the abundance of the gas with a cyclotron frequency equal to applied frequency.

Alpert and Buritz report that an omegatron of this design has a sensitivity of $S = 10/\text{mm Hg}$ which is comparable to that of an ionization gauge. With a magnetic field intensity of 2100 oersteds the RF oscillator must be swept from 3.2 Mc to 81 kc to cover a mass range from 1 to 40. There is some discrepancy between the observed and calculated frequency for a given mass, presumably due to lack of uniformity of the RF field. However, the instrument has adequate resolution up to at least mass 40.

An analysis of the ion motion in the omegatron has been made by Sommer, Thomas, and Hipple [21] assuming a uniform sinusoidal varying RF field normal to a constant magnetic field. The results of their study may be summarized as follows:

Cyclotron or resonant frequency:

$$f = 1.54 \frac{H}{M} \text{ kc.}$$

Number of revolutions made by ions before reaching collector at resonance:

$$n = 3.06 \cdot 10^{-5} \frac{R_0 H^2}{E_0 M} .$$

Time for ions to reach collector at resonance:

$$t = 0.02 \frac{R_0 H}{E_0} \ \mu\text{sec.}$$

Length of spiral path for ions at resonance:

$$L = 9.6 \cdot 10^{-5} \frac{R_0^2 H^2}{E_0 M} \text{ cm.}$$

Final energy of resonant ions at collector:

$$V = 4.8 \cdot 10^{-5} \frac{R_0^2 H^2}{M} \text{ ev.}$$

Maximum radius attained by nonresonant ions differing in mass by the amount ΔM from the resonant ions of mass M:

$$r_m = \frac{2}{\pi n} \frac{M}{\Delta M} R_0 \text{ cm.}$$

Resolution (defined as midpeak frequency per width of resonant peak, theory assumes parallel-sided peaks):

$$\frac{M}{\Delta M} = 4.8 \cdot 10^{-5} \frac{R_0 H^2}{E_0 M} ,$$

where

E_0 = peak value of sinusoidal RF field in v/cm,
M = mass of ion in atomic mass units,
R_0 = distance from electron beam to ion collector in cm, and
H = magnetic field intensity in oersteds.

If these equations are applied to the Alpert and Buritz omegatron it is found that if one assumes $E_0 = 1$ v/cm, $R_0 = 1$ cm and $H = 2100$ oersteds, then for helium the required radio frequency for resonance is 810 kc. At resonance the helium ions will spiral around 34 times traveling about one meter in 42 μsec before being collected. The helium ions will gain 53 ev of energy from the RF field. At the resonance frequency for helium, the molecular ions of hydrogen travel less than 0.4 mm away from the electron beam. The resolution is nearly 53.

The resolution of an omegatron may be improved by operating at low RF voltages. However, under these conditions the ion-path length becomes large and the device must be operated at low pressures to prevent scattering. Further effects of varying the operating parameters on the performance of the omegatron are discussed by Edwards [22].

Magnetic-Deflection Mass Spectrometers

Mass spectrometers of the magnetic-deflection type have also been used in measuring the residual gases in ultra-high vacuum systems. Reynolds [23] has described a high-sensitivity mass spectrometer for noble gas analysis. A nine-stage electron multiplier with magnesium-silver dynodes is used to give a gain in the range of 10^3 to 10^6 electrons per ion. This increase in sensitivity permitted Reynolds to measure partial gas pressures of the order of 10^{-12} mm Hg. A total pressure of 5×10^{-10} mm Hg was achieved during operation of the spectrometer after rigorous bakeouts.

A small, portable, magnetic-deflection-type mass spectrometer with a secondary emission electron multiplier has also been developed by Davis and Vanderslice [24] for studying residual gases at ultra-high vacuums and for making transient pressure studies. This device is shown in Fig. 12. Because of its small size, it has the advantage that it can be sealed directly to the tube or system being investigated and is easily transportable. The spectrometer may be baked out at 450°C and operated at ultra-high vacuums when properly processed.

The design consists of a 90° sector-5-cm radius of curvature magnetic analyzer which will resolve adjacent mass peaks up to about mass 140. A Nier-type ion source is used and the ion detector is a ten-stage DuMont 6467 electrostatically focused electron multiplier

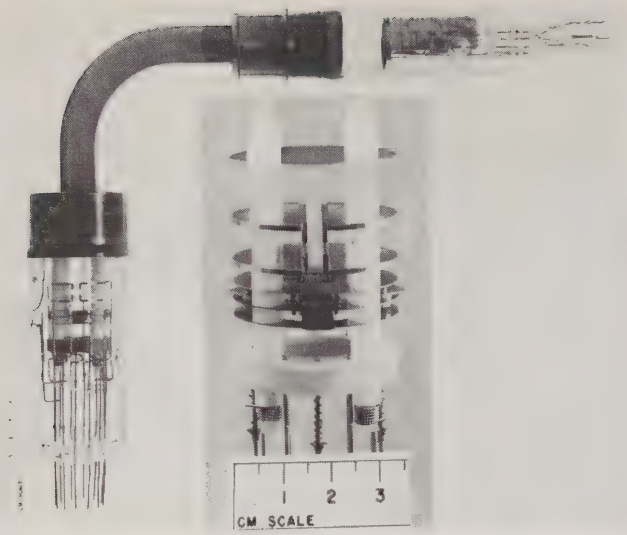

Fig. 12—A small portable mass spectrometer with secondary emission multiplier for the study of transient pressure phenomena at ultra-high vacuums (Davis and Vanderslice).

with a gain of one to ten million. The sensitivity of this spectrometer is in the range of 0.02 to 0.2/mm Hg without the multiplier. Assuming that the lowest current which can be conveniently measured is 10^{-14} a, this spectrometer, without the multiplier, could be used to detect partial pressures of about 10^{-10} mm Hg. With the multiplier, the output current is increased by a factor of 10^6 to 10^7, but because of the multiplier dark current, a gain in sensitivity of only 10^3 can be realized at room temperature. Under normal conditions a dark current of 10^{-10} a was obtained. With a multiplier gain of 10^7 this corresponds to an equivalent ion current of 10^{-17} a. This is equal to the signal current that would be produced by a partial pressure of 10^{-13} mm Hg. Cooling the multiplier in liquid nitrogen or counting individual ion pulses reduces the dark current by a factor of 100, making pressures of the order of 10^{-15} mm Hg measurable.

An additional advantage of the multiplier is that it raises the signal level to a point where a low output load resistance may be used to give a short response time. This makes it possible to scan the mass range and display the spectrum on an oscilloscope. Several ion species may thus be observed almost simultaneously during a transient pressure or composition phenomenon. The saw-tooth voltage which is available on a Tektronix 545 scope and automatically synchronized with the display makes an excellent source of sweep voltage. Fig. 13 shows an example of an oscilloscope display for the isotope spectrum of CO^+ obtained after bakeout at a pressure of 6×10^{-8} mm Hg. The mass peaks 28, 29, and 30 correspond to $C_{12}O_{16}^+$, $C_{13}O_{16}^+$, and $C_{12}O_{18}^+$ respectively. These peaks occur in the ratio 100:1:0.2. This spectrum was taken at a sweep speed of 3 msec per unit mass. Sweep rates as high as 1.5 μsec per unit mass have been used successfully. At the higher sweep rates the familiar well-defined mass peaks degenerate into groupings of pulses due to the collection of individual ions.

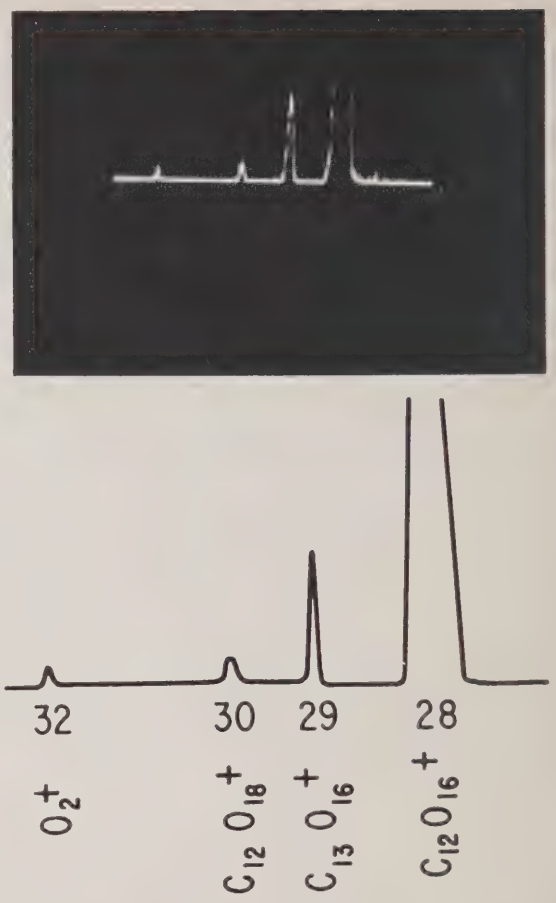

Fig. 13—Oscillogram of CO^+ isotopes taken at 6×10^{-8} mm Hg with a sweep speed of 3 msec/unit mass with the spectrometer shown in Fig. 12.

Vacuum Systems

For any operating vacuum system there will be established a stationary pressure P_e, which corresponds to the equilibrium between the flux of gas into the system and rate of exhaust. This rate of flow of gas Q into the system may arise from desorption from the walls of the system, back diffusion from the pumps, or atmospheric gas permeation of the walls. For a system of volume V and pumping speed S, the rate of reduction of pressure is given by

$$\frac{dP}{dt} = -\frac{S}{V}P + \frac{Q}{V}. \tag{3}$$

For the simple case in which S and Q are constants, independent of pressure, the solution of this equation is

$$P = \frac{Q}{S} + \left(P_0 - \frac{Q}{S}\right)e^{-t/(V/S)}, \tag{4}$$

where V/S is now the pumping-time constant or characteristic pumping time of the system, *i.e.*, the time required to pump the system down to 0.368 of its initial pressure P_0. The equilibrium pressure finally attained in the system will be

$$P_e = \frac{Q}{S}. \tag{5}$$

Obviously, then, to achieve ultra-high vacuum it is necessary that the rate of gas leakage into the system divided by the pumping speed of the system be small.

In order to keep the influx of gas low, it is necessary to keep back diffusion from pumps at a minimum by using effective traps with low-backstreaming pumps.

Desorption from walls of the system is a major source of gas, and this is generally decreased by baking the system to temperatures up to 500°C or by immersing the system in a refrigerant such as liquid helium [25]. The required high-temperature bakeout makes the use of stopcocks, glass taper fittings, wax, etc., impractical.

The leak rate of gas through the walls of the system must be small. Alpert and Buritz [26] have shown that the ultimate limit to the achievement of very low pressures in glass systems is fixed by the diffusion of atmospheric helium through the walls of the system. They measured this rate for borosilicate glass as approximately 10^{-15} mm l/sec/cm^2. A one-liter system with a surface area of 1000 cm^2 would require a pumping speed of only 0.01 l/sec to maintain a pressure of 10^{-10} mm Hg. Norton [27] has made measurements of the permeation rate of helium through various glasses and the results are shown in Fig. 14. The rate for borosilicate glass is in substantial agreement with the value given by Alpert and Buritz.

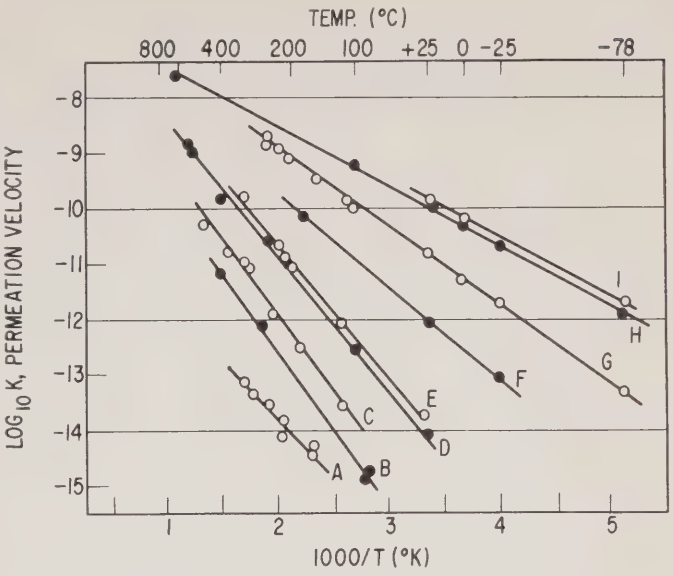

Fig. 14—The log of the permeation velocity K of helium plotted against the reciprocal of the absolute temperature T for various glasses. K is in units of cm^3 gas (NTP/sec/cm^2 area/mm thickness/cm Hg gas-pressure difference). Curve A) Lead borate glass. B) X-ray shield glass. C) Combustion tubing Corning No. 1720. D) Soda-lime glass Corning No. 0080. E) Phosphate glass. F) Borosilicate glass Kimball No. 650. G) Chemical Pyrex-brand glass No. 7740. H) Fused silica. I) Vycor-brand glass.

As the graph shows, the permeation of atmospheric helium can be decreased by a selection of the glass used in the vacuum system. Corning 1720, for example, has a permeation rate 10^{-5} lower than ordinary borosilicate glass (Corning 7740). Since the diffusion rate of helium is much lower through crystalline materials than through glass, it is expected that an all ceramic-metal system would have a low permeation rate for helium and that the ultimate pressure would only be limited by the outgassing of the metal and ceramic.

Another limit to the achievement of low pressures is the finite vapor pressure of the tungsten filament in the ionization gauge. At 2300°K, for example [28], the vapor pressure is 10^{-12} mm Hg. This limits the temperature to which a tungsten filament may be heated in an ultra-high vacuum ionization gauge. However, lanthanum boride [29] produces 10 ma emission at 1000°K and the vapor pressure is about 10^{-4} lower than tungsten at the same electron-emission current density.

In the past few years, a variety of components specifically designed for ultra-high vacuum systems have become available. A discussion of these follows.

Pumps for Ultra-High Vacuum

Diffusion Pumps

The operation of a diffusion pump depends on the effusion of gas molecules from the region being evacuated into the directed vapor stream of the pump [30]. Some of the directed momentum of the vapor molecules is imparted to the gas molecules in the system thus creating a pressure gradient causing the gas to flow through the pump. This process is independent of pressure once the pressure had been lowered by a backing pump to a value at which molecular flow or effusion can occur and the pumping speed will rise to a plateau value and remain there for all lower pressures. The rate of gas evolution from the pump itself becomes significant at lower pressures and eventually exceeds the measured rate of introduction of gases into the pump from the vacuum system. Eventually, then, the net pumping speed of the diffusion pump falls to zero due to the gas evolution and backstreaming of the pump fluid from the pump itself.

Hagstrum [31] and Becker and Hartman [32] at the Bell Telephone Laboratories have used mercury-diffusion pumps with liquid-nitrogen-cooled traps to attain ultra-high vacuum. Recent experiments by Venema and Bandringa [33] have demonstrated that a properly designed mercury pump and a series of traps will attain a vacuum of at least 10^{-12} mm Hg. Vanderslice has achieved a pressure of 3×10^{-12} mm Hg at room temperature using the techniques of the above authors.

Oil diffusion pumps have very high pumping speeds, but until recently it was felt that their pressure limit was in the vicinity of 10^{-7} mm Hg. Even with a high pumping speed, the ultimate pressure is limited by the high value of backstreaming. Alpert [34] has shown that at some pressure between 10^{-7} and 10^{-8} mm Hg the conventional oil diffusion pump becomes a source of contamination for a "clean" vacuum system. The oil pumps were at first used to evacuate the systems down to 10^{-7} mm Hg and after the system was closed off from the oil pumps, the pumping action of the ionization gauge was

used to pump to lower pressures. Alpert [35] subsequently designed a copper-foil trap, shown in Fig. 15, that would prevent the backstreaming of oil vapor but would not seriously restrict the conductance and pumping speed of the system. With the gettering action of the copper-eliminating backstreaming, the oil pump evacuated the system to pressures below 10^{-10} mm Hg. The copper-foil trap was effective even at room temperature and for periods of several months. The trap was reactivated by baking with the rest of the system. The exact mechanism whereby the trap adsorbs backstreaming oil vapor at room temperature is not fully understood, but with proper traps an oil diffusion pump may be used in ultra-high vacuum experiments.

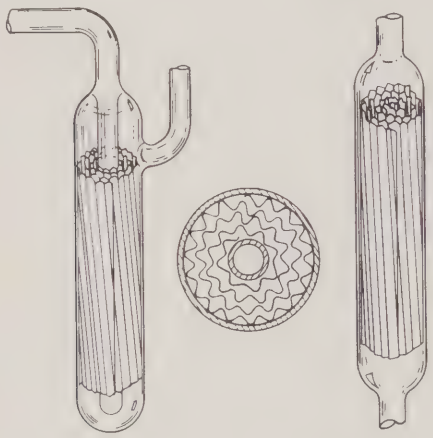

Fig. 15—Copper-foil trap (Alpert).

The recent work of Biondi [36] utilizing nonrefrigerated molecular sieve traps has had, and will continue to have, a profound impact on the use of oil pumps for ultra-high vacuum experiments. With these traps it is now possible to achieve ultra-high vacuum with oil pumps without the use of refrigerants for reasonably long times. The most popular materials at the moment are zeolite and alumina with some advantages being claimed for alumina. Harris [37] has demonstrated that the activity of oxide cathodes may be maintained for a period of several days, and perhaps longer with the use of alumina traps. A comparative test without alumina and with conventional cold trapping showed that a similar oxide cathode lost much of its activity in a comparable time.

Ion Pumps

The ionization gauge itself may be used for pumping, once the pressure has been brought to a low value.The pumping speed of ionization gauges is low, of the order of hundredths of liters per second, but with a low influx of gas Q the speed is sufficient for a well-baked-out system. Alpert [38] has demonstrated that a Bayard-Alpert gauge with titanium continually evaporated to the wall has a pumping speed of at least 20 liters/sec at low pressures.

The most important development in the last few years has been the advent of commercially available ion pumps with relatively high pumping speeds down to at least 10^{-9} mm Hg. Hall [39] reports a pressure of 10^{-11} mm Hg using a baked-metal system and an ion pump.

The cold-cathode ion pump is basically a variation of a Penning ionization gauge consisting of a ring anode and two cathode plates in a magnetic field as shown in Fig. 4. The anode is operated at high-positive potential with respect to the cathode. Electrons emitted by the cold cathode are forced into a spiral path by the presence of a strong magnetic field. The increased electron path results in a high probability for collision and ionization between electrons and gas molecules. The positive ions then bombard the cathode and sputter metal from the cathode. The sputtered metal deposits in various regions of the tube forming stable compounds with the chemically active gas molecules. Chemically inert gas atoms such as argon are also pumped, but by a different mechanism. In an ion pump much of the inert gas is initially found in the sputtered deposit on the cathode. Fig. 16 shows a radiograph of the cathode of a commercial two-electrode pump in which radioactive krypton 85 has been pumped. The pump was disassembled and the cathode placed in contact with a photographic film showing that the krypton was chiefly located in the sputtered deposit on the cathode.

If the ion current density on an electrode surface is uniform, the clean-up of inert gas on that surface is zero after a short period of time. Initially a small number of ions will be imbedded in the surface, but as soon as sputtering occurs, imbedded gas is released. A condition is soon reached in which the net clean-up rate is zero since the rate at which ions are driven into the newly exposed surface is just equal to the rate of release of gas from the surface by sputtering. If an ion current density gradient exists on the electrode surface, there will be a build-up of sputtered metal in areas of low current density and consequently gas clean-up will occur. The Penning-type discharge in a two-electrode pump is somewhat unstable during operation, producing changes in the distribution of the ion current density at the cathode surface. This results in the resputtering of previously sputtered metal on the cathode, and consequently in the release of gas previously cleaned up. This is frequently referred to as the ion pump memory effect. This effect is reported to be minimized by grooving the cathode [40].

Inert gases are also cleaned up at the anode to some extent [40], [41]. The gas is found in the metal which has been sputtered from the cathode. There is the question how the gas sticks to the anode since unexcited inert gas atoms are not adsorbed on the electrode surfaces for long enough times at room temperature to be covered by sputtered metal and the ions normally do not have sufficient kinetic energy to reach the anode. There are several plausible explanations for this: 1) neutral inert gas atoms are excited by the discharge stick

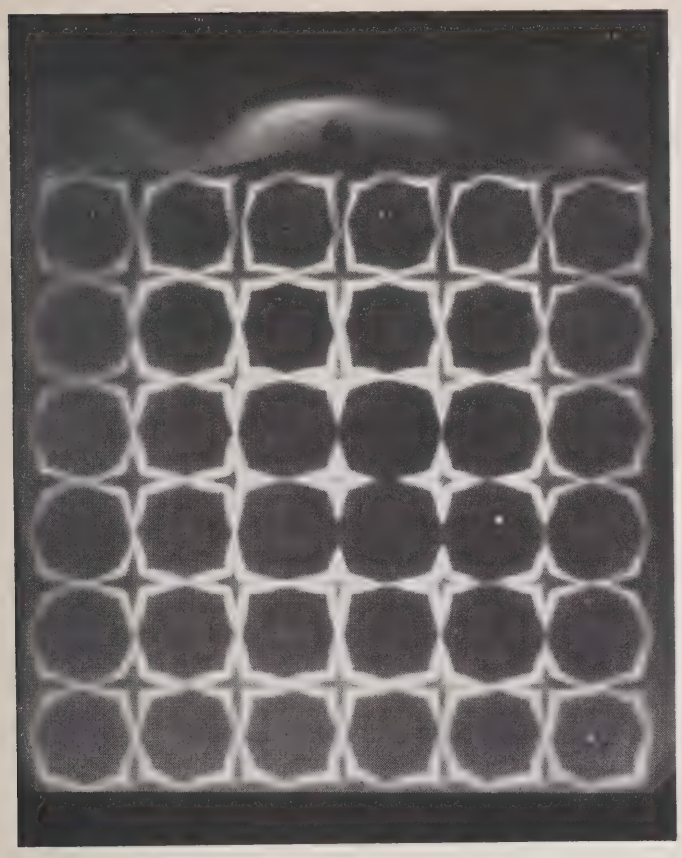

Fig. 16—Radiograph showing the location of radioactive krypton 85 in the sputtered deposit on the cathode of an ion pump.

to the anode and are covered by sputtered metal from the cathode; 2) high-velocity neutral atoms produced by charge exchange are driven into the anode and then covered by sputtered metal from the cathode; 3) the gas ions gain sufficient kinetic energy to reach the anode through oscillations in the discharge; and 4) the gas is swept out of the space between the electrodes by the high flux of the metal vapor. The first two explanations appear more likely. Although the anode mechanism is less efficient than coverage of ions at the cathode, the clean-up is permanent because resputtering of material from the anode cannot occur.

Three-electrode ion pumps have been studied in this laboratory [41] and elsewhere [42]. In the arrangement shown in Fig. 17, the third electrode is placed in a favorable position to receive sputtered metal from the cathode. The voltage applied to this electrode is intermediate between the cathode and anode so that the inert gas ions are driven into it with sufficient energy to be embedded but not sufficient to cause appreciable sputtering. Thus gas cleaned up by this electrode is permanent.

Ion pumps offer great promise of replacing many conventional diffusion pumps. Their principal advantages are that the system is never exposed to contamination from diffusion-pump fluids and no refrigerants are necessary. One of their present disadvantages is the difficulty of pumping large quantities of organic vapors of high molecular weight such as benzene and toluene at pressures above 10^{-5} mm Hg. Another disadvantage is their inability continually to pump large amounts of gas at high pressure because of excessive cathode heating and sputtering.

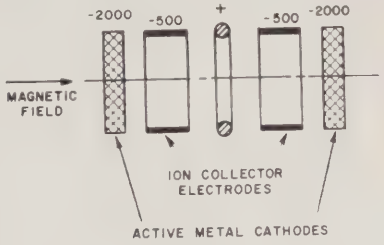

Fig. 17—Three-electrode ion pump.

Cryogenic Pumps

Immersion of the whole or part of a vacuum system in liquid air or immersion of a trap containing charcoal in liquid air was a convenient way of producing low pressures in the days before the advent of diffusion pumps. In recent years with the need for large systems for space simulation and routine experiments at ultra-high vacuum, cryogenic pumping is again becoming popular. At liquid-helium temperatures, only helium and hydrogen have appreciable vapor presseses. All other gases condense out on the surface of the cooled container. The sticking probability for most gases approaches unity as the temperature is lowered, and the total pressure can be reduced to the ultra-high vacuum range in the absence of hydrogen or helium. If hydrogen or helium are present in quantities greater than monolayer amounts, they can be removed by other means such as ion pumping. The speed of a cryogenic pump is determined by the area of the cold surface and the conductance of the connecting tubing.

For the efficient design of a cryogenic pump, it is necessary to reduce the radiation incident on the trap from the walls of the vessel. The helium trap is normally jacketed by liquid nitrogen.

Cryogenic pumping shows much promise for large specialized system applications such as space-simulation chambers. The General Electric Missile and Space Vehicle Department in Philadelphia, Pa., is constructing a gigantic space simulator using low-temperature gaseous helium-cooled walls as pumps.

Ultra-High Vacuum Components

Since mercury cutoffs, standard stopcocks, and rubber gaskets are not bakeable, their use in ultra-high vacuum systems is prohibited. Stopcock grease, mercury or other fluids used in cutoffs tend to contain large amounts of occluded gas. This has led to the development of a new line of hardware components for ultra-high vacuum systems.

Vacuum Tubes

Alpert [35] has developed a tube (Fig. 18) which can withstand bakeout at ~450°C and has a sufficiently large conductance for ultra-high vacuum systems. Since then there have been many improvements in this general type of tube [43]. A popular commercially available tube is made by the Granville-Phillips Corporation of Pullman, Wash., and is shown in Fig. 19. This particular tube has a conductance variable from one liter/sec to less than 10^{-14} liter/sec.

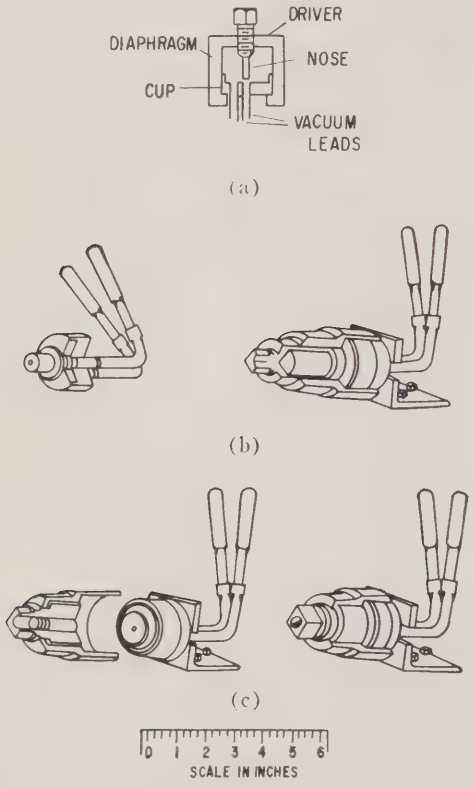

Fig. 18—Ultra-high vacuum bakeable metal valve (Alpert). (a) Schematic diagram. (b) Tube with differential screw-driving mechanism. (c) Tube with simple screw-driving mechanism.

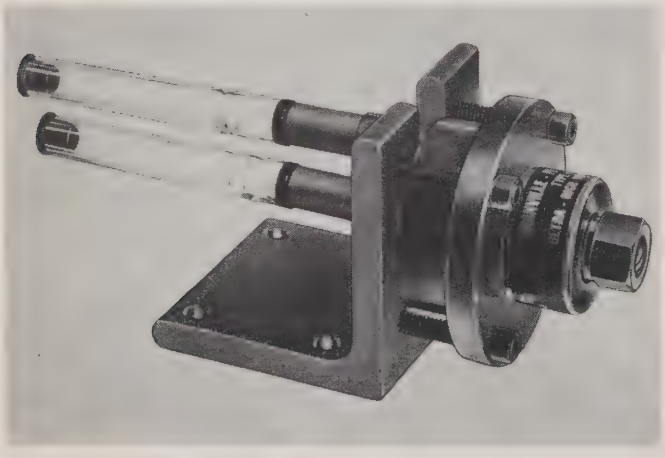

Fig. 19—Granville-Phillips tube.

Molten-metal tubes are becoming more popular [44]. The advantage of this type of tube over ordinary mercury cutoffs is that the metal is a solid at room temperature having a low vapor pressure. The metal is raised into the seal-off position while the tube is hot and then is allowed to solidify by cooling and this completes the seal. They lack some of the convenience of other types of tubes, but have the advantage of simplicity.

Demountable Seals

The convenience of a demountable seal is often desired even in an ultra-high vacuum device. The usual device consists of a metal gasket crushed between two flanges [35], [45]. The gasket metal is selected for its ductility as well as its low vapor pressure at bakeout temperatures. Pattee [46] described a demountable joint which was used in a field-emission apparatus. The seal (Fig. 20) consists of a knife edge which seats in an annealed copper gasket. The knife edge is machined on heavy wall stainless-steel tubing. It has a 0.005-inch radius at the tip and a 45° wedge angle. Adjustment is permitted by deformation of the copper by the clamping screws.

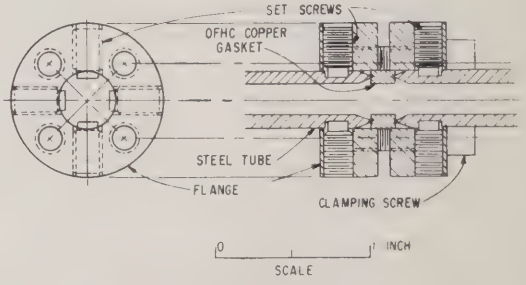

Fig. 20—Demountable vacuum seal (Pattee).

Modern Vacuum Systems

A major requirement of an ultra-high vacuum system is that the system be capable of being baked at high temperatures. This is most conveniently done by having a furnace placed around the entire vacuum system. There are many possible arrangements and one which has been found convenient in this laboratory is shown in Fig. 21. Two walls of the oven are fixed permanently in place. These can be made of insulated stainless-steel or asbestos board. The vacuum components, such as tubes, are attached directly to the surface with flexible glass bellows or long glass U bends inserted between each fixed point. Lightweight insulated aluminum modular ovens are placed over the system during bakeout and the temperature is controlled by any convenient pyrometer. Only a number of the heating units (Calrods) is controlled by the pyrometer and the others are controlled manually. If it is desired to bring the system quickly to temperature, the manually-controlled Cal-

rods are turned on. When the bakeout temperature is approached, these heating units are turned off and the automatically-controlled Calrods maintain the temperature in the vicinity of the desired value. The automatically-controlled heating units do not have enough power to heat the oven more than 50°C above the desired temperature. In this manner, if the controller fails to function, there is less danger of melting the glassware. In practice, however, the automatically-controlled heaters are used to bring the furnace to temperature in a few hours.

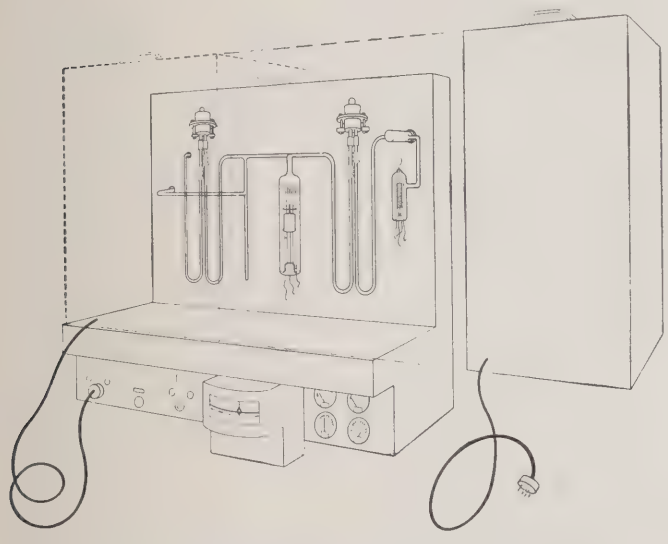

Fig. 21—Typical laboratory ultra-high vacuum system.

The procedure is much the same whether mercury, oil or ion pumps are used. The system is first pumped to $\sim 10^{-6}$ mm Hg and a cursory check for leaks is made. The ovens are usually placed over the system and the automatic controller is set to the desired temperature. The entire system, including the traps, back to the pumps is baked at 425°C. After four or five hours at 425°C, the furnace on the trap closest to the pump is shut off. With mercury pumps, the trap is cooled by a Dewar filled with liquid nitrogen. When alumina traps are used in conjunction with oil diffusion pumps, the trap is simply allowed to cool to room temperature. With ion pumps no trap is needed. A common procedure is to use two ion pumps in sequence, one of which is baked out and the other is used to pump the system during bakeout. When mercury or oil pumps are used the system is kept hot for approximately four hours after the traps have cooled before allowing to cool slowly to room temperature. The ovens are removed and the pressure of the system is checked with an ionization gauge, and a check is made for small leaks. The detection of leaks is quite simple in the pressure range below 10^{-8} mm Hg. Acetone and carbon tetrachloride, for example, applied to a small leak cause the positive-ion current reading on the ionization gauge to increase suddenly, or they clog the leak temporarily and cause the current to decrease. Helium and hydrogen can also be used with success. Measurement of the rate of rise of pressure also will detect a leak, and by shutting off various sections of the system, the leak can be isolated. Final pin-pointing is usually done with the ionization gauge. If no leaks are found, the metal parts are outgassed at high temperatures by electron bombardment or by RF heating. In some cases a second bakeout is done after the outgassing and pressures of 10^{-10} mm Hg are routinely obtained.

Leak Detectors

To the experimenter interested in using vacuum systems, one of the greatest problems is leaks. Leaks may occur from a variety of causes, and the increasing complexity of tube design has multiplied the number of these causes to a great extent. The time-honored method of detecting leaks in glass systems by means of a Tesla spark coil has become obsolete with all-metal vacuum systems. Leak detectors involving a change in thermionic emission caused by an adsorbed layer of gas on the filament of a diode or ionization gauge have been used successfully as described in the previous section. The present trend in leak detection is towards the sensitive high-speed helium mass spectrometer. The development of a new leak detecting process using radioactive gas has made it possible to detect leaks in sealed systems or devices without destruction or opening to air. Some of the leak detectors of current interest are described below.

Mass Spectrometers

A very sensitive method for the detection of leaks, and one which also gives an indication in a minimum of time, was developed by Jacobs and Zuhr [47]. It involves the use of a mass spectrometer with helium [48], and the principle by which it operates may be described briefly as follows: When a beam of positive ions, accelerated by a potential V, is passed through a magnetic field of strength H, the ions are sorted out according to their values of e/m, where m is the mass of the ion and e the charge. The radius of curvature R of the path of any given type of singly-charged ion is determined by

$$R = 143.9 \frac{\sqrt{MV}}{H}, \qquad (6)$$

where R is expressed in centimeters, V in volts, H in oersteds, and M is the molar mass of the ion in grams.

For example, for $R = 4.0$ cm and $H = 1500$ oersteds, the values of V for helium ($M = 4.003$) and nitrogen ($M = 14.008$, since N^+ is formed), are found to be 434 and 124 v, respectively. Thus, for a given value of the radius of curvature, the ions reaching a collector may be differentiated by varying the value of V, and the mag-

nitude of the ion current at any given voltage setting will depend on the concentration of the ions in the beam, that is, on the rate at which the corresponding molecules leak into the spectrometer.

For the detection of leaks, helium has been chosen as testing gas for the following reasons:

1. Because of the low value of M, the rate of diffusion through a leak is greater than that of any other gas except hydrogen.
2. Helium occurs in the atmosphere to the extent of only one part in 200,000 parts of air.
3. There is little possibility that an ion due to any other gas will give an indication that can be mistaken for helium.

The application of the mass spectrometer to the detection of leaks has been described in two papers, one by Worcester and Doughty [49] and the other by Thomas, Williams, and Hipple [50].

A modern version of the helium mass spectrometer leak detector is shown in Fig. 22. This instrument is capable of detecting leaks as small as 10^{-10} cc of air per sec in evacuated enclosures. Such a leak is so small that more than 5000 years would be required for one cubic inch of air at atmospheric pressure to pass through the opening. For pressurized enclosures leaks down to 10^{-6} cc per sec can be located. In this spectrometer the helium ions are deflected through 90° by the magnetic field. The current generated by collection of the helium ions is amplified and used to indicate a leak on the leak-rate meter and on an audible alarm. The components to be leak checked are connected to a manifold which is first exhausted by the mechanical roughing pump, and when the pressure, as indicated, for instance, by a thermocouple gauge connected to the test manifold is sufficiently low the throttle valve to the spectrometer tube is opened. A fine jet of helium is passed over suspected parts in each of the tubes, and the presence of a leak is indicated on the leak-rate meter.

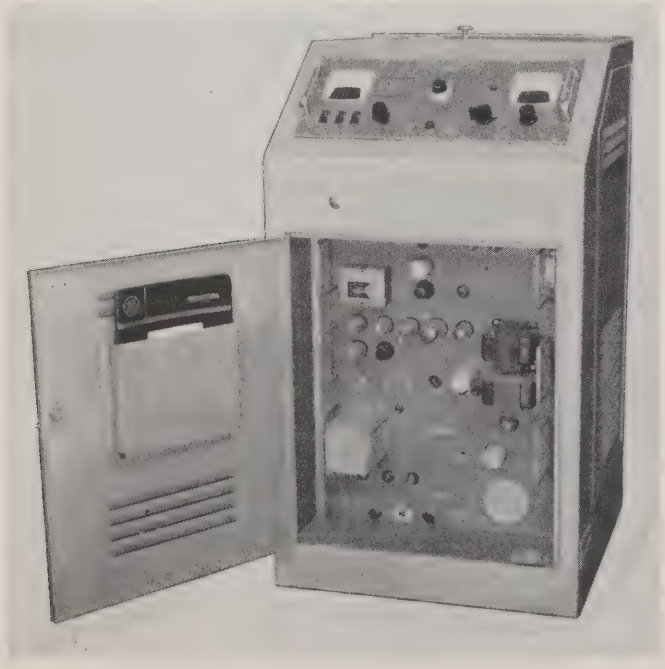

Fig. 22—Mass-spectrometer leak detector (General Electric, M-60).

Fast leak testing is made possible with this spectrometer by the incorporation of an automatic balance circuit. This circuit allows the leak detector to respond only to a rapid increase in helium signal such as obtained when a jet of helium passes near a leak. When large systems are being tested, large leaks are sometimes encountered with the jet of helium which cause the mass-spectrometer vacuum system to become partially saturated with helium. Normally, the operator would have to wait a considerable time before the helium has been pumped out of the system to a point where leak testing can be resumed. However, with the automatic balance circuit the helium background is balanced out and a leak signal is given only when the operator passes the jet of helium near a leak.

Radiflow Method

A new method of leak testing hermetically-sealed components nondestructively by utilizing a radioactive gas has been described by Cassen and Burnham [51]. Leakage rates in the order of 10^{-12} cc per sec can be measured under favorable conditions by this process called "radiflo." Equipment for this leak detection system is manufactured by the Analytical and Control Division of Consolidated Electrodynamics Corporation, Pasadena, Calif. The basic principle involves the detection of radioactive krypton 85 which has been allowed to diffuse into the leaky components. Krypton 85 has a half-life of 10.3 years. Over 99 per cent of the disintegrations involve the emission of beta rays with a maximum energy of 0.67 Mev, while only 0.7 per cent of the disintegrations give 0.54-mev gamma rays. The gamma emitting disintegrations are used to detect the leaks since the gamma rays will pass readily through most materials. Detection of the beta rays may be used under some circumstances to determine the presence of occluded krypton on the surface of the components under test. The testing procedure is as follows: The components to be tested are placed in an activating tank which is then sealed. Air in the tank is evacuated down to approximately 2 mm Hg and diluted krypton 85 is pumped into the tank under pressure up to 7 atmospheres. The radioactive gas diffuses into existing leaks in the components. After a prescribed "soaking" period, which may be from several minutes to a few hundred hours, the krypton is pumped out of the activating tank and returned to storage for reuse. If the leaks follow Poiseuille's Law, the quantity of krypton diffusing into leaky components will increase with the square of the pressure and linearly with time. Thus a suitable combination of krypton pressure and "soaking" time may be selected to give the desired sensitivity. Next, an air wash is circulated over the components to remove any residual krypton from the external surfaces. The com-

ponents are then removed from the activating tank. Those with leaks will retain some radioactive atoms which emit gamma radiation. This radiation is detected by a scintillation counter and the intensity is determined by a ratemeter. When this radiation intensity is related to the conditions of the activation process, the leak rate may be determined.

Some components may have absorptive surfaces such as organic coatings, gaskets, or insulation which will retain krypton 85 for various lengths of time after the pressure is released. The gamma radiation emitted by this absorbed gas could make the components appear as leakers when, in fact, they are not. A routine check of rejected parts with a thin-window Geiger-Müller counter tube for beta ray activity reveals surface contaminations.

Halogen-Ion Detector

Quite different in principle from all the other methods of leak detection described above is that involved in the positive-ion detector for halogen compounds which has been described by White and Hickey [52].

Some of the earliest investigators in the field of thermionic emission, such as O. W. Richardson, had observed that platinum, even in air at a temperature of a red heat, emits positive ions, and that the rate of ion emission increases with temperatures according to a relation similar to that observed for electron emission from incandescent cathodes. This positive-ion emission is probably due mostly to the presence in the anode of salts of the alkali metals, although this may not be the correct interpretation of the mechanism of operation of the device described below.

It was observed by C. W. Rice of the General Electric Company that this emission, at any given anode temperature, of positive ions in air is increased very markedly when vapors of compounds containing a halogen strike the electrode surface. This observation forms the basis of the detector developed and described by White and Hickey.

A diagrammatic sketch of the device and simple circuit used for its operation are shown in Fig. 23. The detector consists of a platinum cylinder P which is heated by an insulated platinum filament F, the low voltage required for this purpose being supplied by the transformer T. A metal cylinder C, concentric with P, is connected through a microammeter (μA) to the negative end of a dc source of voltage (50–500 v) while P is connected through the midpoint of the secondary of T to the positive end of the voltage source.

In using the device for detection of leaks, air or any other suitable gas containing a halogen vapor is introduced into the system at a positive pressure. This positive pressure forces the air containing the halogen out through the leak where it may be picked up by the device and is indicated by the meter in the detector circuit. Or the detector may be sealed on the vacuum system in series with the pump (preferably between the rough and the fine pumps). Air containing a halogen vapor is forced under pressure through a very small jet and directed at any suspected spot in the system and then is picked up by the detector.

In using the detector, the temperature of the anode should be between 850°C and 950°C. At lower temperatures, the positive-ion emission is too small, and at higher temperatures the emission becomes unstable. Typical halogen compounds which are fairly volatile at room temperatures and therefore applicable in using the positive-ion detector are "Freon," carbon tetrachloride, and chloroform.

A convenient form of the halogen-leak detector is shown in Fig. 24. The unit contains a power supply, amplifier, sensing element and an air pump. The detector probe is connected to the control unit through a flexible cable. Air drawn in at the probe passes through

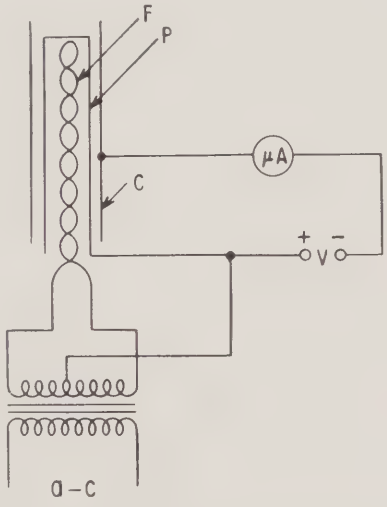

Fig. 23—Schematic diagram of the thermionic detector and circuit used for detection of halogen compounds (White and Hickey).

Fig. 24—Gun-type halogen leak detector (General Electric, H-2).

the sensing element and is exhausted through the pump. When the probe is moved so as to pass near a leak, the sudden increase of halogen gas mixing with the air going into the probe will cause an increase in the detector ion emission. This current is amplified and measured on the leak-rate meter. The detector may be used to locate leaks down to 5×10^{-5} cc/sec in an atmosphere with contamination up to 1000 parts of halogen gas per million parts of air.

The halogen-leak detector has a special advantage in that no helium is required. This has given this method preference in instances where scarcity of helium has been a problem [53].

Bibliography

[1] O. E. Buckley, "An ionization manometer," *Proc. Natl. Acad. Sci. U. S.*, vol. 2, pp. 683–685; 1916.
[2] S. Dushman and C. G. Found, "Studies with the ionization gauge," *Phys. Rev.*, vol. 17, pp. 7–19; January, 1921.
[3] J. D. Cobine, "Gaseous Conductors," Dover Publications, Inc., New York, N. Y., p. 81; 1958.
[4] G. J. Schulz and A. V. Phelps, "Ionization gauges for measuring pressures up to the millimeter range," *Rev. Sci. Instr.*, vol. 28, pp. 1051–154; December, 1957.
[5] F. M. Penning, "Ein Neues Manometer für Niedrige Gasdrucke, Insbesondere Zwischen 10^{-3} und 10^{-5} mm," *Physica*, vol. 4, pp. 71–75; February, 1937.
[6] ——, and K. Nienhuis, "Construction and applications of a new design of the Philips vacuum gauge," *Philips Tech. Rev.*, vol. 11, pp. 116–122; October, 1949.
[7] J. R. Downing and G. Mellen, "A sensitive vacuum gauge with linear response," *Rev. Sci. Instr.*, vol. 17, pp. 218–223, June, 1946; also G. L. Mellen, "Radium-type vacuum gage," *Electronics*, vol. 19, pp. 142–146, April, 1946.
[8] N. W. Spencer and R. L. Boggess, "A radioactive ionization gage pressure measurement system," *J. Am. Rocket Soc.*, vol. 29, pp. 68–71; January, 1959.
[9] W. B. Nottingham, "Comments on Vacuum Gauges," presented at the 7th Annual Conf. on Phys. Electronics, Mass. Inst. Tech., Cambridge; March, 1947.
[10] R. T. Bayard and D. Alpert, "Extension of the low pressure range of the ionization gauge," *Rev. Sci. Instr.*, vol. 21, pp. 571–572; June, 1950.
[11] L. Apker, "Surface phenomena useful in vacuum technique," *Ind. Engrg. Chem.*, vol. 40, pp. 846–847; May, 1948.
[12] W. B. Nottingham, "Design and Properties of the Modified Bayard-Alpert Gauge," in "Vacuum Symposium Transactions," Committee on Vacuum Techniques, Inc., Boston, Mass.; pp. 76–80; 1954.
[13] D. Alpert, "New developments in the production and measurement of ultra high vacuum," *J. Appl. Phys.*, vol. 24, pp. 860–876; July, 1953.
[14] W. B. Nottingham, "A Detailed Examination of the Principles of Ion Gauge Calibration," presented at the Am. Vacuum Soc. Symp., Cleveland, Ohio; October, 1960.
[15] J. P. Hobson and P. A. Redhead, "Operation of an inverted magnetron gauge in the pressure range 10^{-3} to 10^{-12} mm Hg," *Can. J. Phys.*, vol. 36, pp. 271–288; March, 1958.
[16] P. A. Redhead, "The Townsend discharge in a coaxial diode with axial magnetic field," *Can. J. Phys.*, vol. 36, pp. 255–270; March, 1958.
[17] J. M. Lafferty, "Hot-cathode magnetron ionization gauge for the measurement of ultrahigh vacua," *J. Appl. Phys.*, vol. 32, pp. 424–434; March, 1961; U. S. Patent No. 2,884,550; October 17, 1957.
[18] G. K. T. Conn and H. N. Daglish, "A thermionic ionization gauge of high sensitivity employing a magnetic field," *J. Sci. Instr.*, vol. 31, pp. 412–416; November, 1954.
[19] H. Sommer, *et al.*, "The measurement of e/M by cyclotron resonance," *Phys. Rev.*, vol. 82, pp. 697–702; June, 1951.
[20] D. Alpert and R. S. Buritz, "Ultra-high vacuum. II. Limiting factors on the attainment of very low pressure," *J. Appl. Phys.*, vol. 25, pp. 202–209; February, 1954.
[21] H. Sommer, *et al.*, "The measurement of e/M by cyclotron resonance," *Phys. Rev.*, vol. 82, pp. 697–702; June, 1951.
[22] A. G. Edwards, "Some properties of a simple omegatron-type mass spectrometer," *Brit. J. Appl. Phys.*, vol. 6, pp. 44–48; February, 1955.
[23] J. H. Reynolds, "High sensitivity mass spectrometer for Noble gas analysis," *Rev. Sci. Instr.*, vol. 27, pp. 928–934; November, 1956.
[24] W. D. Davis and T. A. Vanderslice, "A Sensitive, High-Speed Mass Spectrometer for Ultrahigh Vacuum Work," presented at the Am. Vacuum Soc. Symp., Cleveland, Ohio; October, 1960.
[25] P. A. Redhead and E. V. Kornelsen, "High vacuum techniques," *Vakuum-Tech.*, in press.
[26] D. Alpert and R. S. Buritz, "Ultra-high vacuum. II. Limiting factors on the attainment of very low pressure," *J. Appl. Phys.*, vol. 25, pp. 202–209; February, 1954.
[27] F. J. Norton, "Helium diffusion through glass," *J. Am. Ceram. Soc.*, vol. 36, pp. 90–96; March, 1953.
[28] D. Alpert and R. S. Buritz, "Ultra-high vacuum. II. Limiting factors on the attainment of very low pressure," *J. Appl. Phys.*, vol. 25, pp. 202–209; February, 1954.
[29] J. M. Lafferty, "Boride cathodes," *J. Appl. Phys.*, vol. 22, pp. 299–309; March, 1951.
[30] G. W. Sears, "Ultimate vacua of diffusion pumps," *Rev. Sci. Instr.*, vol. 20, pp. 458–459; June, 1949.
[31] H. D. Hagstrum, "Electron ejection from Mo by He^+, He^{++}, and He_2^+," *Phys. Rev.*, vol. 89, pp. 244–255; January, 1953.
[32] J. A. Becker and C. D. Hartman, "Field emission microscope and flash filament techniques for the study of structure and adsorption on metal surfaces," *J. Phys. Chem.*, vol. 57, pp. 153–159; February, 1953.
[33] A. Venema and M. Bandringa, "The production and measurement of ultra-high vacua," *Phillips Tech. Rev.*, vol. 20, pp. 145–157; December, 1958.
[34] D. Alpert, "New developments in the production and measurement of ultra high vacuum," *J. Appl. Phys.*, vol. 24, pp. 860–876; July, 1953.
[35] ——, "Vacuum valve for the handling of very pure gases," *Rev. Sci. Instr.*, vol. 22, pp. 536–537; July, 1951.
[36] M. A. Biondi, "High-speed nonrefrigerated isolation traps for ultra-high vacuum systems," *Rev. Sci. Instr.*, vol. 30, pp. 831–832; September, 1959.
[37] L. A. Harris, "Trapping with alumina in vacuum systems and its effect on cathode activity," *Rev. Sci. Instr.*, vol. 31, pp. 903–904; August, 1960.
[38] D. Alpert, "Recent advances in ultra-high vacuum technology," *Vacuum*, vol. 9, pp. 89–96; May, 1959.
[39] L. D. Hall, "Ionic vacuum pumps," *Science*, vol. 128, pp. 279–285; August, 1958.
[40] R. L. Jepsen, *et al.*, "Stabilized Air Pumping with Diode Type Getter-Ion Pumps," presented at the Am. Vacuum Soc. Symp., Cleveland, Ohio; October, 1960.
[41] K. B. Blodgett and T. A. Vanderslice, "Mechanism of Argon Cleanup in a Gas Discharge," presented at Gaseous Electronics Conf., New York, N. Y.; October, 1958.
[42] W. M. Brubaker, "A Method for Greatly Enhancing the Pumping Action of a Penning Discharge," 6th Natl. Symp. on Vacuum Tech., pp. 302–306; October, 1959.
[43] D. Alpert, "Production and measurement of ultrahigh vacuum," in "Handbuch der Physik," vol. 12, Springer Verlag, Berlin, Germany; 1958.
[44] For example, see N. N. Axelrod, "Ultrahigh-vacuum valve," *Rev. Sci. Instr.*, vol. 30, pp. 944–945; October, 1959.
[45] H. Hintenberger, "Erfahrungen mit Metallfolien als Hochvakuumdichtungen," *Z. Naturforsch.*, vol. 6a, pp. 459–462; 1959.
[46] H. H. Pattee, "A demountable ultra-high vacuum joint," *Rev. Sci. Instr.*, vol. 25, pp. 1132–1133; November, 1954.
[47] R. B. Jacobs and H. F. Zuhr, "New developments in vacuum engineering," *J. Appl. Phys.*, vol. 18, pp. 34–48; January, 1947.
[48] A. O. Nier, *et al.*, "Mass spectrometer for leak detection," *J. Appl. Phys.*, vol. 18, pp. 30–33; January, 1947.
[49] W. G. Worcester and E. G. Doughty, "High vacuum leak testing with the mass spectrometer," *Trans. Am. Inst. Elect. Engrs.*, vol. 65, pp. 946–955; December, 1946.
[50] H. A. Thomas, *et al.*, "A mass spectrometer type of leak detector," *Rev. Sci. Instr.*, vol. 17, pp. 368–372, October, 1946; also "Detecting vacuum leaks electronically," *Westinghouse Engr.*, vol. 6, pp. 108–110, July, 1946.
[51] B. Cassen and D. Burnham, "A method of leak testing hermetically sealed components utilizing radioactive gas," *Intern. J. Appl. Radiation and Isotopes*, vol. 9, pp. 54–59; December, 1960.
[52] W. C. White and J. S. Hickey, "Electronics simulates sense of smell," *Electronics*, vol. 21, pp. 100–102; March, 1948.
[53] A. Weber, "Lecksucher nach dem Halogenverfahren für Hochvakuumröhren," *Glas- u. Hochvakuum-Tech.*, vol. 2, pp. 259–262; September, 1953.

GENERAL ELECTRIC

Research Laboratory

SCHENECTADY, N. Y.

5-61 (50M)